



City Research Online

City, University of London Institutional Repository

Citation: Guo, L., Liu, Y., Fu, F. & Huang, H. (2019). Behavior of axially loaded circular stainless steel tube confined concrete stub columns. *Thin-Walled Structures*, pp. 66-76. doi: 10.1016/j.tws.2019.02.014

This is the accepted version of the paper.

This version of the publication may differ from the final published version.

Permanent repository link: <https://openaccess.city.ac.uk/id/eprint/21730/>

Link to published version: <https://doi.org/10.1016/j.tws.2019.02.014>

Copyright: City Research Online aims to make research outputs of City, University of London available to a wider audience. Copyright and Moral Rights remain with the author(s) and/or copyright holders. URLs from City Research Online may be freely distributed and linked to.

Reuse: Copies of full items can be used for personal research or study, educational, or not-for-profit purposes without prior permission or charge. Provided that the authors, title and full bibliographic details are credited, a hyperlink and/or URL is given for the original metadata page and the content is not changed in any way.

Behavior of axially loaded circular stainless steel tube confined concrete stub columns

Lanhui Guo^{a *}, Feng Fu^b, Yong Liu^a, Haijia Huang^a

^a School of Civil Engineering, Harbin Institute of Technology, Harbin, China

^b School of Mathematics, Computer Science & Engineering, City, University of London, EC1V 0HB, U.K.

Abstract: A stainless steel tube confined concrete (SSTCC) stub column is a new form of steel-concrete composite column in which the stainless steel tube without bearing the axial load directly is used to confine the core concrete. It could take the advantages of both the stainless steel tube and the confined concrete columns. This paper presents the experimental investigation of circular SSTCC stub columns subjected to axial load. Meanwhile, comparative tests of the circular concrete-filled stainless steel tubes and circular hollow stainless steel tubes were also conducted. The experimental phenomena of specimens are introduced in detail and the experimental results are analyzed. Through the investigation of axial stress and circumference stress on the stainless steel tube, the interaction behavior between stainless steel tube and core concrete is studied. The experimental results showed that the stainless steel tube provides better confinement to the concrete core, thus results the compressive capacity increased obviously comparing with unconfined concrete. The load-carrying capacity of SSTCC stub columns is higher than that of concrete-filled stainless steel tubes. An equation to calculate the load-carrying capacity of SSTCC stub columns was proposed, the results based on calculation are close to the experimental results.

Keywords: Stainless steel tube; steel tube confined concrete; stub columns; axially loaded; experimental study.

* Corresponding author.
E-mail address: guolanhui@hit.edu.cn

23 Notations

A_c	Cross-sectional area of the concrete core
A_s	Cross-sectional area of stainless steel tube
D	Out-diameter of stainless steel tube
E_s	Elastic modulus of stainless steel
E_s^t	Tangent modulus on the plastic stage of stainless steel
f_{cu}^{100}	Compressive strengths of 100 mm concrete cubes
f_{ck}	Compressive strengths of 150 mm concrete cubes
f_r'	Effective confining stress of circular tube on the concrete
f_p	Yield stress of stainless steel
N_s	Axial force on stainless steel tube
N_c	Axial force resisted by core concrete
N_{ue}	Ultimate compressive strength of specimen
t	Thickness of stainless steel tube
$\sigma_{0.2}$	Stress in accordance to 0.2% of plastic strain for stainless steel
σ_h	Hoop stress on stainless steel tube
σ_v	Vertical stress on stainless steel tube
σ_z	Equivalent stress on stainless steel tube
ε_h	Hoop strain on stainless steel tube
ε_v	Vertical strain on stainless steel tube
μ_s	Poisson's ratio of stainless steel
μ_{sp}	Poisson's ratio for the stainless steel in the plastic stage

24 1. Introduction

25 The conventional carbon steel tube confined concrete columns is a type of steel-concrete composite
 26 column, in which the steel tube is discontinuous at the beam-column joints to ensure no axial load is
 27 imposed directly to the tube [1-3]. Fig.1 shows the steel tube confined concrete columns. Concrete-filled
 28 steel tubes as a kind of composite column are widely studied and used in the buildings. The main difference
 29 between steel tube confined concrete columns and concrete filled steel tubes is that the steel tube is cut at
 30 both end near to beam column connection for steel tube confined concrete members. If the steel tube is cut

on both ends, the steel tube would not resist the vertical load directly, thus the confinement to the core concrete is better than that of concrete-filled steel tubes. Meanwhile, for steel tube confined concrete columns, the beam-column connection is easy for the construction of rebar and pouring concrete if reinforced concrete beam is applied. During the past decades, sufficient researches [4-8] have been conducted on the behaviors of the steel tube confined concrete columns, which indicates that such type of members has relatively high bearing capacity, good ductility as well as excellent fire resistance. In addition, the steel tube can act as the formwork during the construction stage, making it easier to cast the concrete. Due to the excellent mechanical and manufacture properties, steel tube confined concrete columns are used increasingly in projects, especially in the Middle East and the east Asia. Fig.2 shows the application of circular steel tube confined concrete columns used in Zhongke Tower, Chongqing. This 26-storey building will be finished in 2019. The height of this building is 99.80 m.

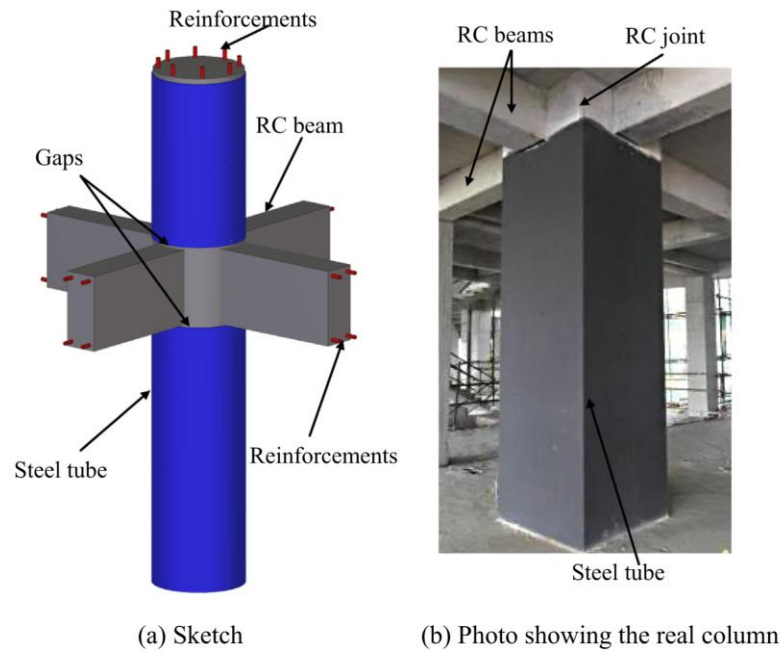


Fig.1. Steel tube confined concrete columns



Fig.2. Zhongke Tower

Using stainless steel tube is another innovation for steel tube confined concrete columns. Apart from the advantages mentioned above, the stainless steel tube confined concrete (SSTCC) columns also have the extra benefits such as the fine aesthetic appearance and high corrosion resistance associated with the material of stainless steel. Unlike carbon steel, stainless steel possesses natural corrosion resistance. Thus, after being appropriately processed, the surface can be exposed without any protective coatings. Besides, stainless steel also exhibits features, such as the ease of maintenance, ease of construction and high fire resistance compared to traditional carbon steel. Therefore, stainless steel could be used in steel tube confined concrete column to enhance its durability.

In the past, experimental and theoretical studies have been conducted on the behaviors of carbon steel tube confined concrete columns, which included axially loaded behavior, eccentric loaded behavior and seismic behavior. The square and circular shape cross-sections were both studied. Based on these studies, the methods to calculate loading-carrying capacities of carbon steel tube confined concrete columns were proposed [9-11].

Compared to the carbon steel, stainless steel has a stress-strain curve with no yield plateau and low proportional limit stress. The ductility of stainless steel is much better than that of carbon steel. Because of

the advantageous and different properties of stainless steel, some researchers such as Young and Elloboldy [12-14] studied the behavior of concrete-filled stainless steel tube (CFSST) columns. A series of tests were conducted to investigate the effects of the shape of stainless steel tube, plate thickness and concrete strength on the behavior and strength of axially loaded CFSST columns. Dennis and Leroy [15] tested eight CFSST columns and eight concrete filled carbon steel tube columns with square section. They also compared the strengths of those members with that determined by the existing design methods for composite carbon steel sections in Eurocode 4 and ACI 318. In addition, a new method to predict the axial capacity of concrete filled stainless steel hollow sections was also developed. In 2013, Hassanein et al. [16] performed finite element analysis on the behavior of CFSST columns. Suliman et al [17] tested thirty-five concrete-filled stainless steel tubular columns to investigate the effect of different parameters on their behavior. Two concrete compressive strengths of 44 MPa and 60 MPa and three diameter-to-thickness ratios of 54, 32, and 20 were considered. The axially loaded behavior of concrete-filled stainless/carbon steel double skin columns were done by Ye, Han and Wang [18-20]. Feng and Chen did a series of research works about CFSST columns, which includes the bond behavior between tube and concrete and the flexural behavior of the members [21-24].

The above literature review indicates that past studies were mainly focused on carbon steel tube confined concrete columns or concrete-filled stainless steel tube columns. Currently, little research has been conducted on SSTCC columns. As it has been discussed, stainless steel can be used to replace carbon steel for enhancing the durability of steel tube confined concrete columns. However, limited experimental investigations were presented in available literatures focusing on the performance of axially loaded SSTCC columns.

To understand the behavior of SSTCC columns clearly, a series of tests were conducted under axial

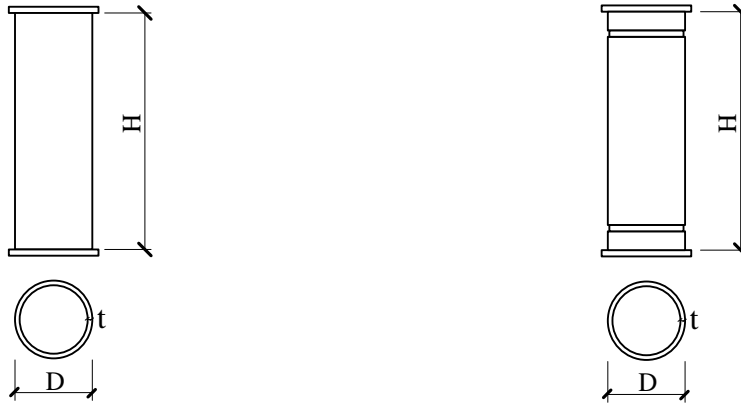
compression. For comparison purposes, concrete-filled stainless steel tubular columns and hollow stainless steel tubes were tested. At last, an equation to calculate the load-carrying capacity of SSTCC columns subjected to axial load was suggested.

2. Experimental study

2.1. Test specimens

In order to understand the behaviors of stainless steel tube confined concrete (SSTCC) columns, 18 specimens were tested under monotonic loaded axial compression load using the 5000 kN capacity high-stiffness compression machine at the structural lab in Harbin Institute of Technology. Among 18 specimens, nine of them are stainless steel tube confined concrete stub columns, six specimens are concrete filled stainless steel stub columns, and three specimens are hollow stainless steel tubes columns. All specimens are stub columns with a height-to-diameter ratio of 3.0 to eliminate the end effect and column slenderness effect. The dimensions of all specimens are presented in Fig. 3 and Table 1. Two kinds of thicknesses of steel plate are selected, which are 1.3 mm and 1.65 mm. The diameter-to-thickness ratio varies from 89 to 109.

All the tubes employed were produced by rolling the steel plate to circular members, and then weld the steel tube by butt weld. A rigid end plate with 10 mm thickness was welded to the bottom of the tube. The concrete was filled into the tube and after 28 days of curing, another rigid steel plate was covered and welded to the top of the tube. The surface of end plates was smooth and flat after grinding using a grinding wheel with diamond cutters. This was to ensure that the load was applied evenly across the cross-section and simultaneously to the steel tube and the core concrete. To insure the axial load is applied to the core concrete only in SSTCC columns, two 10 mm wide girth strips were cut off from the steel tube at 30 mm away from the end plates, as shown in Fig. 3.



(a) Concrete filled stainless steel tube columns

(b) Stainless steel tube confined concrete members

Fig.3. Dimension of the specimen

Table 1 Geometric and material properties of specimens

Specimens	H /mm	D /mm	t /mm	D/t	$\sigma_{0.2}$ /MPa	f'_c /MPa
SSTCC-D125-a	374.5	125.3	1.29	97	496	54.5
SSTCC-D125-b	374.9	124.8	1.25	100	496	54.5
SSTCC-D125-c	374.8	124.5	1.33	94	496	54.5
CFSST-D125-a	375.3	124.8	1.31	95	496	54.5
CFSST-D125-b	374.5	125.3	1.30	96	496	54.5
SST-D125-a	375.5	124.8	1.31	96	496	--
SSTCC-D150-a	444.9	149.7	1.63	92	493	54.5
SSTCC-D150-b	444.8	149.8	1.67	90	493	54.5
SSTCC-D150-c	445.1	150.2	1.67	90	493	54.5
CFSST-D150-a	444.8	150.1	1.68	89	493	54.5
CFSST-D150-b	444.9	149.8	1.65	91	493	54.5
SST-D150-a	445.0	150.2	1.66	90	493	--
SSTCC-D180-a	540.4	180.8	1.68	108	493	54.5
SSTCC-D180-b	540.5	180.6	1.65	109	493	54.5
SSTCC-D180-c	539.8	180.7	1.67	108	493	54.5
CFSST-D180-a	539.7	180.7	1.69	107	493	54.5
CFSST-D180-b	540.4	180.7	1.70	106	493	54.5
SST-D180-a	539.9	180.8	1.70	106	493	--

Note: In the nomenclature of the group, ‘SSTCC’ is the abbreviation of circular stainless steel tube confined concrete; ‘CFSST’ is the abbreviation of circular concrete-filled stainless steel tubes; ‘SST’ is the abbreviation of circular hollow section stainless steel tubes. “D125” means the nominal diameter of the specimen is 125 mm while “a” is the number for the specimen of the same type.

2.2. Material properties

The stainless steel employed in the specimen is the austenitic stainless steel with the section of ASTM (American Society for Testing and Materials) 304. In order to determine the property of stainless steel, three tensile coupons were cut from a randomly location of the selected steel sheet. The coupons were made and tested in accordance with the Chinese standard GB/T 228-2002 [25]. Typical tensile stress-strain curve of stainless steel is presented in Fig. 4. As can be seen, the stress-strain curve of the stainless steel has no yield plateau and good ductility.. For steel plates with thickness of 1.3 mm and 1.65 mm, the elastic modulus of steel plates were $2.17 \text{ E}+5 \text{ N/mm}^2$ and $2.15 \text{ E}+5 \text{ N/mm}^2$, and the average yielding strengths were 496 N/mm^2 and 493 N/mm^2 , respectively.

When casting concrete, three concrete prisms with dimension of $150 \text{ mm} \times 150 \text{ mm} \times 300 \text{ mm}$ were casted and cured in the same conditions as the specimens. The test procedure was in accordance to the Chinese standard GB/T 50081-2002 [26]. The average compressive strength of concrete was 54.5 N/mm^2 . The average modulus of concrete was 38100 N/mm^2 .

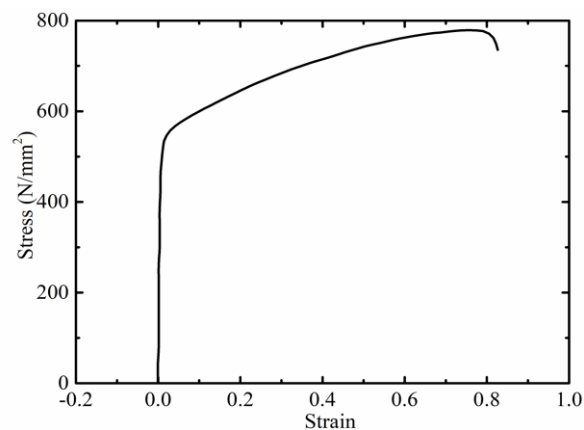
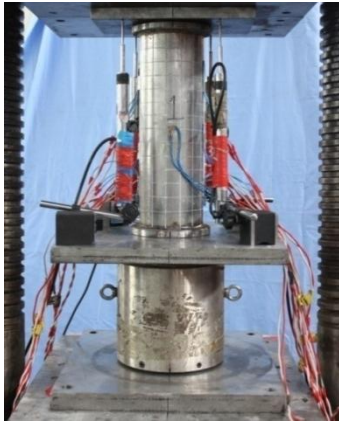


Fig.4. Strain-stress relationship of stainless steel with thickness of 1.3 mm

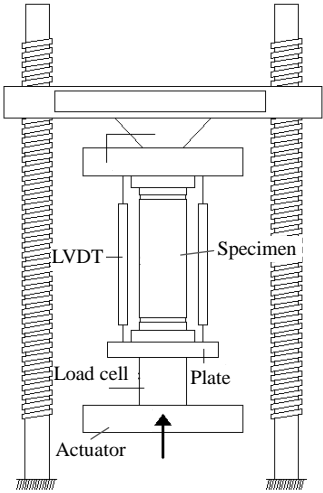
2.3. Experimental setup and load schedule

As shown in Fig. 5 and Fig. 6, eight strain gauges were stuck at the mid-height on each face of the specimen, which were arranged in the longitudinal and transverse directions with 90° angles. Four

displacement transducers were used to measure the axial deformation. Fig. 5 illustrates the experimental setup.



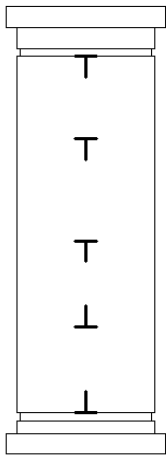
(a) Photo of test setup



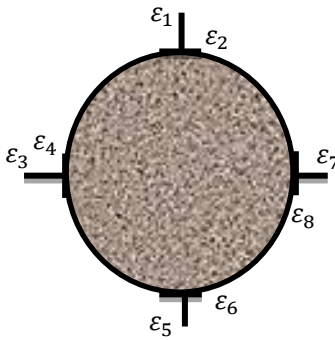
(b) Diagram of setup

Fig.5. Experimental setup

The tests were conducted using a 5000 kN capacity universal testing machine in Harbin Institute of Technology, and the load was applied directly on the specimen. The tests were firstly loaded with controlled increment of the rate of 0.06MPa/s. When the yielding of specimen starts (the maximum strain reaches the yielding strain of steel plate), the loading process turned into the displacement control with the rate of 10 $\mu\epsilon$ /s. The tests were terminated when the axial load decreased to 75% of the peak load caused by fracture of steel plate or crushing of concrete.



(a) Side view of columns



(b) Section at mid-height



(c) End and quartile section

Fig.6. Location of strain gauges

3. Experimental phenomena

3.1. Stainless steel tube confined concrete stub columns

During the initial loading stage, no significant changes were observed. Before the axial load reached 80% of peak load, the relationship between axial load and deformation was kept as linear, and the specimen was in the elastic stage. After the load exceeded 80% of peak load, the axial displacement started to quickly increase with the increasing of axial load. When the axial load reached 98% of peak load, small cracking appeared at the position of cutting of steel tube. When the specimen reached the peak load, the concrete at the cutting position of steel tube spalled. Then the axial load decreased slowly with the increasing of axial deformation. When the axial load decreased to 85% of peak load, the lateral deflection of steel tube was observed, and the steel tube was slightly bloated without significant local buckling. To observe the damage of core concrete, the steel tubes were cut off and removed after the test. It is noticed that the core concrete fails in shear failure mode with severe cracks along the diagonal direction. The angle between shear failure plane and the horizontal direction is about $45^{\circ}\sim 49^{\circ}$. The experimental phenomena of typical specimens are shown in Fig.7. For specimens with diameter of 150 mm, when the axial load decrease to 93% from the peak load, the steel tube at the position of welding broke, thus the load started to decrease sharply. The reason was that the steel tube cannot provide confinement to the core concrete any more. Therefore, it is noticeable that, the quality of longitudinal weld is very important for this type of structural members, especially for the sake of sufficient ductility of the specimen.



(a) Phenomena of specimen SSTCC-D125-a

(b) Phenomena of specimen SSTCC-D150-b

Fig.7. Failure mode of stainless steel tube confined concrete members

3.2. Concrete-filled stainless steel tubular columns

For concrete-filled stainless steel tubular columns, the phenomena of all specimens were similar to each other. Taken specimen CFSST-D125-b as an example, the phenomena and failure mode were introduced in the following. Before the axial load reached 80% of peak load, there was no evident phenomenon on the surface of the specimen. The relationship between axial load and vertical deformation kept linear. When the specimen reached 80% of peak load, the stiffness of axial load-deformation relationship curve began to decrease. The local bulge of steel tube was observed near the bottom (about 50 mm from end plate). The bulge gradually increased with the increase of vertical deformation. The peak load of the specimen was 1142 kN, and the corresponding vertical displacement was 2.72 mm. When the specimen decreased to 95% of peak load, the steel tube bloated at the mid-height position. When the axial load decreased to 90% of peak load, the axial load decreased very slowly with the increase of vertical deformation. The specimen exhibited global shear failure mode. The angle between shear failure plane and horizontal plane was located between 48° ~ 53° . The experimental phenomena were shown in Fig. 8.



(a) Phenomena of specimen CFSST-D125-a (b) Phenomena of specimen CFSST-D150-b

Fig. 8 Failure mode of concrete-filled stainless steel tubes

3.3. Hollow stainless steel tubes with circular section

According to the Eurocode 3 ‘Design of Steel Structures, Part 1-4: General rules-Supplementary rules for stainless steels’, if the diameter-to-thickness ratio (D/t) ratio is over $90 \cdot 235 / \sigma_{0.2} \cdot E_s / 210000$, the local buckling would appear for circular hollow stainless steel sections before the steel reaches its yielding strength. According to the Chinese Technical specification for stainless steel structures, if the diameter to thickness ratio is over $100 \cdot 235 / \sigma_{0.2}$, the local buckling of circular hollow section stainless steel stub would be considered. Considering the yielding stress of stainless steel of 493 N/mm^2 , the limit diameter-to-thickness ratios for local buckling are 42.9 and 47.7 according to EC 3 code and Chinese design code, respectively. In the test, for specimens with diameter of 125 mm, 150 mm and 180 mm, the corresponding diameter-to-thickness ratios are 96, 90 and 106, respectively. It can be seen that the circular stainless steel tube would fail in the elastic stage.

For stainless steel hollow section, at the initial loading stage, there is no evident phenomenon for these specimens. The axial load-deformation relationship kept linear before the specimens reached 80% of their bearing capacity. Beyond this, the deformation increased significantly with the increase of axial load. The rigidity of axial load-deformation relationship curve began to decrease. When the specimen reached its

peak load, the inward local buckling near the bottom occurred accompanied by a sudden drop of the load-carrying capacity and the increase of vertical displacement. The reason was that the specimen failed at the elastic stage of steel. From these specimens, it can be seen that severe buckling ripples appeared on the steel tubes. The experimental phenomena are shown in Fig. 9. When the load dropped to 50% of peak load, the vertical deformation reached the 1/50 of the specimen height. The test was terminated.



Fig.9. Experimental phenomena of stainless steel tubes with circular hollow section

4. Experimental results analysis

4.1. Interaction behavior between steel tube and core concrete

4.1.1. Strain-stress relationship of stainless steel under biaxial stresses

In 2008, Quach, Teng and Chung [27] developed three-stage strain stress relationship formula which is based on the extensive theoretical and experimental research works. In this paper, the authors further modified the formula based on the regression of the test results of stainless steel coupons presented in this paper. The modified formulae are coincided well with the strain-stress relationship of stainless steel. The formulae are as follows:

$$\varepsilon = \begin{cases} \sigma/E_s & (\sigma \leq f_p) \\ \frac{\sigma}{E_s} + 0.002 \left(\frac{\sigma}{\sigma_{0.2}} \right)^n & (f_p < \sigma \leq \sigma_{0.2}) \\ \frac{\sigma - \sigma_{0.2}}{E_s} + \left[0.008 + (\sigma_{1.0} - \sigma_{0.2}) \left(\frac{1}{E_s} - \frac{1}{E_{0.2}} \right) \right] & (\sigma_{0.2} < \sigma \leq \sigma_{1.0}) \\ \left(\frac{\sigma - \sigma_{0.2}}{\sigma_{1.0} - \sigma_{0.2}} \right)^{n'_{0.2,1.0}} + \varepsilon_{0.2} & (\sigma_{0.2} < \sigma \leq \sigma_{1.0}) \\ \frac{\sigma - \sigma_{1.0}}{k_2 E_s} + \varepsilon_{1.0} & (\sigma > \sigma_{1.0}) \end{cases} \quad (1)$$

Where, ε is the strain of stainless steel;

σ is the stress of stainless steel;

E_s is the initial elastic modulus of stainless steel;

f_p is the yield stress of stainless steel, and $f_p = k_1 \sigma_{0.2}$;

$\sigma_{0.2}$ is the nominal yield stress in accordance to 0.2% plastic strain;

$E_{0.2}$ is the tangent modulus corresponding to nominal yield stress of $\sigma_{0.2}$, $\frac{E_{0.2}}{E_s} = \frac{1}{1 + 0.002n/e}$;

n is the strain hardening index, $n = \frac{\ln(20)}{\ln(\sigma_{0.2}/\sigma_{0.01})}$;

e is the coefficient, $e = \frac{\sigma_{0.2}}{E_s}$;

For stainless steel, k_1 is taken as 0.35, k_2 is taken as 0.02;

$\sigma_{1.0}$ is calculated according to $\sigma_{1.0}/\sigma_{0.2} = 0.542/n + 1.0$.

The stress analysis method from reference [28] is used in this paper. Different to CFSST, for SSTCC columns, the stainless steel tube would confine the lateral expansion of core concrete. In reality, the stress in radial direction of stainless steel tube is very small, which can be neglected. Thus, the stainless steel tube is assumed to be under the state of hoop tensile stress combining with axial compressive stress. According to the lateral and longitudinal strain of the stainless steel tube obtained from the tests, the axial stress σ_v , hoop stress σ_h and equivalent stress σ_z on the stainless steel tube can be calculated based on the

assumptions that:

- the stress in the radial direction of the tube is ignored;
- thin plate theory is used for the tube, therefore, the circumference stress is presumed evenly distributed along the thickness of the wall;
- the concrete core is under the axial and radius stress states;
- no slips are presumed between the tube and the concrete core.

The stress-strain relationships of stainless steel for each stage is as follows:

1) In the elastic stage, the stainless steel follows the Hooke's Law:

$$\begin{bmatrix} \sigma_h \\ \sigma_v \end{bmatrix} = \frac{E_0}{1-\mu_s^2} \begin{bmatrix} 1 & \mu_s \\ \mu_s & 1 \end{bmatrix} \begin{bmatrix} \varepsilon_h \\ \varepsilon_v \end{bmatrix} \quad (2)$$

Where, μ_s is the Poisson's ratio for stainless steel.

2) In the plastic stage, the stainless steel follows Elastic-Plastic theory:

$$\begin{bmatrix} \sigma_h \\ \sigma_v \end{bmatrix} = \frac{E_s^t}{1-\mu_{sp}^2} \begin{bmatrix} 1 & \mu_{sp} \\ \mu_{sp} & 1 \end{bmatrix} \begin{bmatrix} \varepsilon_h \\ \varepsilon_v \end{bmatrix} \quad (3)$$

Where, E_s^t is the secant modulus.

$$E_s^t = \begin{cases} 1 / \left[\frac{1}{E_0} + \frac{0.002n \left(\frac{\sigma}{\sigma_{0.2}} \right)^{n-1}}{\sigma_{0.2}} \right] & f_p \leq \sigma < \sigma_{0.2} \\ 1 / \left[\frac{1}{E_{0.2}} + \frac{\left[0.008 + (\sigma_{1.0} - \sigma_{0.2}) \left(\frac{1}{E_0} - \frac{1}{E_{0.2}} \right) \right] n'_{0.2,1.0} \left(\frac{\sigma - \sigma_{0.2}}{\sigma_{1.0} - \sigma_{0.2}} \right)^{n-1}}{\sigma_{1.0} - \sigma_{0.2}} \right] & \sigma_{0.2} \leq \sigma \leq \sigma_{1.0} \end{cases} \quad (4)$$

μ_{sp} is the Poisson's ratio of stainless steel in the plastic stage,

$$\mu_{sp} = 0.167 \frac{\sigma_p^f}{f_y f_p} + 0.283 \quad (5)$$

3) In the strain hardening stage

$$\begin{bmatrix} \sigma_h \\ \sigma_v \end{bmatrix} = \frac{E_s}{Q} \begin{bmatrix} \sigma_v'^2 + 2p & -\sigma_v' \sigma_h' + 2\mu_s p \\ -\sigma_v' \sigma_h' + 2\mu_s p & \sigma_h'^2 + 2p \end{bmatrix} \begin{bmatrix} \varepsilon_h \\ \varepsilon_v \end{bmatrix} \quad (6)$$

Where, σ_v' is the axial stress, $\sigma_v' = \sigma_v - \sigma_{cp}$;

σ_h' is the circumference stress, $\sigma_h' = \sigma_h - \sigma_{cp}$;

σ_{cp} is the average stress, $\sigma_{cp}=1/3 (\sigma_h + \sigma_v)$;

$$p = \frac{2H'}{9E_s} \sigma_z^2 \quad (7)$$

$$H' = \frac{d\sigma}{d\epsilon_p} = 10^{-3} E_s^2 \quad (8)$$

σ_z is the equivalent stress, $\sigma_z = \sqrt{\sigma_h^2 + \sigma_v^2 - \sigma_h \sigma_v}$;

$$Q = \sigma_h^2 + \sigma_v^2 + 2\mu_s \sigma_h \sigma_v + \frac{2H'(1-\mu_s)}{9G} \sigma_z^2;$$

When the stress such as σ_v , σ_h and σ_z are calculated, the internal force of the tube and the concrete core can be calculated correspondingly.

The axial force resisted by the stainless steel tube N_s :

$$N_s = \sigma_v A_s \quad (9)$$

Where, A_s is the cross-sectional area of the tube; σ_v is the axial stress of the tube.

The axial stress of the concrete σ_c can also be derived as

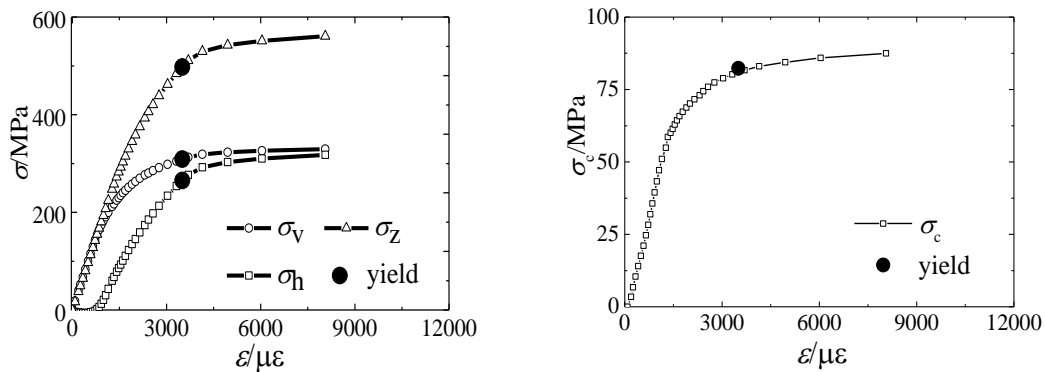
$$\sigma_c = (N - N_s) / A_c \quad (10)$$

Where, N is the axial load of the specimen; A_c is the cross-sectional area of core concrete.

4.1.2. Interaction behaviour of stainless steel tube and core concrete for SSTCCs

Based on the above calculation method, the vertical stress and horizontal stress on the stainless steel tube for SSTCC members can be calculated. Fig. 10 shows the average stress and strain relationship curves at the mid-height of the specimen. In Fig. 10 (a), the symbol σ_v denotes the axial average stress, the symbol σ_h denotes the circumference stress, and the σ_z denotes the equivalent stress. For comparison of the values, the axial stress σ_v (compressive stress) defines as positive values. In the elastic stage, the axial stress σ_v increased with the increasing of axial strain, and the circumference stress σ_h is nearly about zero. The axial stress is resulted from the friction between steel tube and core concrete. Thus the steel tube at the mid-height of the specimen would resist the axial stress. The mechanism of SSTCC column is similar to that of the concrete-filled steel tube columns. In this stage, the circumference deformation of concrete is

very small and the interaction behavior between stainless steel tube and concrete is not obvious. When the axial strain ε_v reached 850 $\mu\epsilon$, the corresponding stress of core concrete was equal to 39.4 MPa. At this point, the average stress of core concrete reached the compressive strength of concrete. Beyond this point, the circumference stress increased sharply with the increasing of axial strain. When the equivalent stress reached the stress of $\sigma_{0.2}$, the corresponding axial stress and circumference stress are 309 MPa and 265 MPa, respectively. Under different strain level, the load resisted by the steel tube can be calculated, then the load resisted by the core concrete can be calculated by subtracting the load resisted by stainless steel tube from the total axial load. Fig. 10 (b) shows the average axial strain-stress relationship curve of core concrete. It can be seen that when the steel tube reached its yielding stress, the average compressive stress of core concrete reached 85 MPa, which is much higher than the maximum compressive stress of 54.5 MPa of unconfined concrete. This is due to the tube confinement to the core concrete.



(a) Axial stress vs. strain on stainless steel tube (b) Axial stress vs. strain of the core concrete

Fig.10. Average stress and strain relationship curves of specimen SSCCT-D125-a

4.1.3. Interaction behaviour of stainless steel tube and core concrete for CFSSTs

The axial stress-strain relationship curves on the stainless steel tube of concrete-filled stainless steel tubes are shown in Fig. 11 (a). It can be seen that the axial stress of steel is almost same to the equivalent stress when the axial strain of steel is less than 3000 $\mu\epsilon$. In addition, the circumference stress of steel is

negative value, which means the steel tube is under compression along the circumference direction. The reason was that the Poisson's ratio of concrete is smaller than that of steel. The radial deformation of steel is larger than that of concrete. However, the cohesion between steel and concrete restrained the radius deformation of steel tube. Thus the circumference stress of steel tube appeared as axial stress. With the increasing of axial strain, the Poisson's ratio of concrete became larger than that of steel. The expansion deformation of core concrete became larger than that of steel. The stainless steel tube would confine the deformation of core concrete. When the equivalent stress reached the yield stress of stainless steel, the circumference stress on the steel tube is 50 MPa. The core concrete is under the state of three-directional compression. The compressive stress of core concrete reached 75 MPa, which is higher than that of concrete without confinement. Besides, the compressive stress of core concrete in CFSST columns is smaller than that in SSTCC columns indicating that the confinement of stainless steel tube in CFSST columns is smaller than that in SSTCC columns.

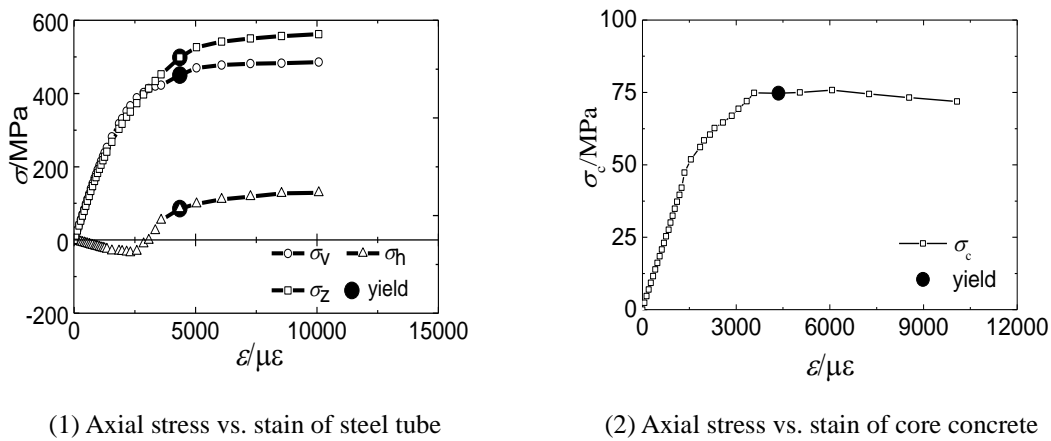


Fig.11. Average stress and strain relationship curves of specimen CFSST-D150-1

4.2. Axial load-strain relationship curves

Fig. 12 and Fig. 13 show the axial load-strain relationship curves of SSTCC stub columns and CFSST. For SSTCC stub columns, the axial strain is defined as the axial deformation divided by the height of the specimen. It can be seen that the rigidity and load-carrying capacity of each group of specimens with same

286 parameters are close to each other. The deformation ability of CFSST stub columns is better than that of
 287 SSTCC stub columns. The reason was that the circumference stress of SSTCC stub columns is larger than
 288 that of CFSST columns. The failure of the welding on SSTCC stub columns resulted in the early failure of
 289 the specimens. Hence, for SSTCC columns, the hot-rolled stainless steel tubes are suggested to be used in
 290 the construction.

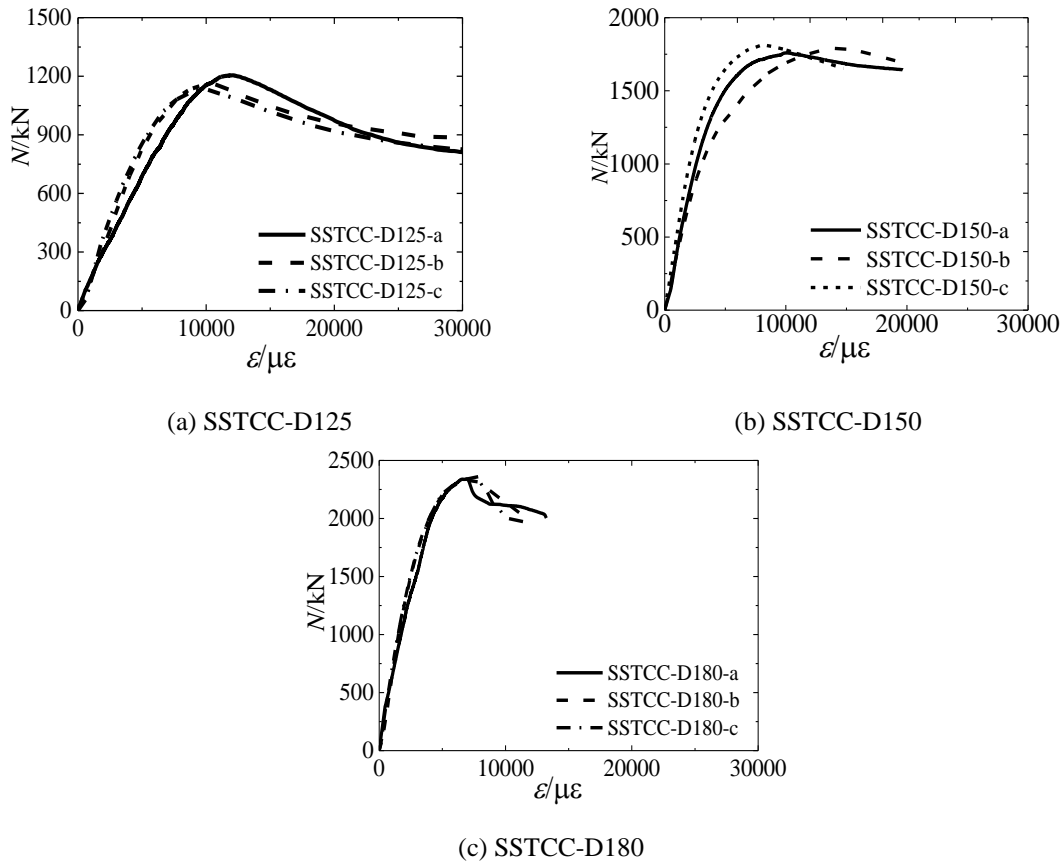
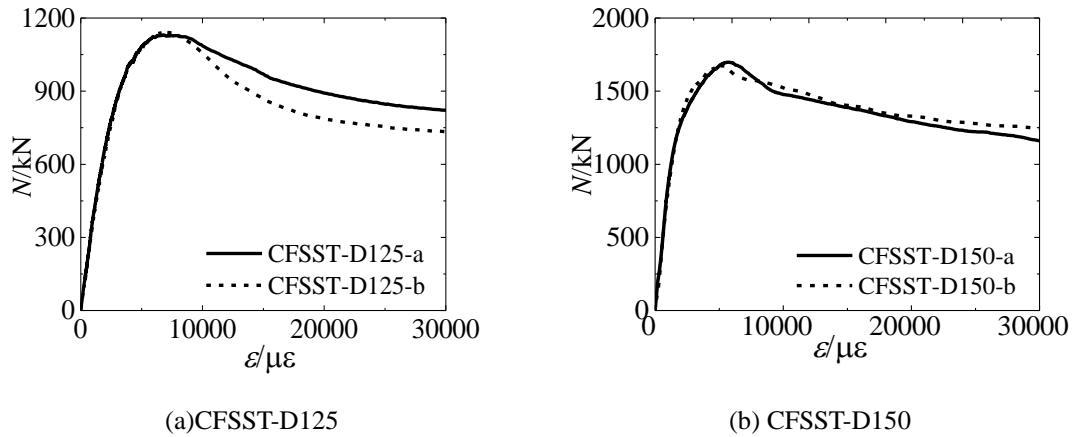
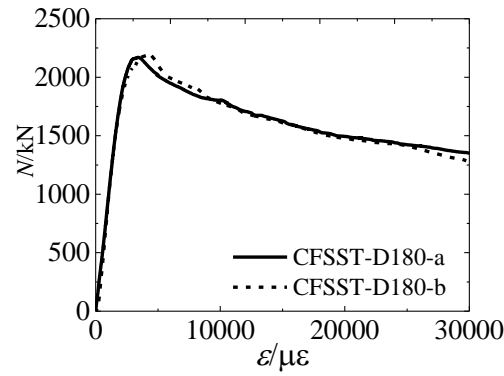


Fig. 12. Axial strain vs. axial load relationship of SSTCC stub columns





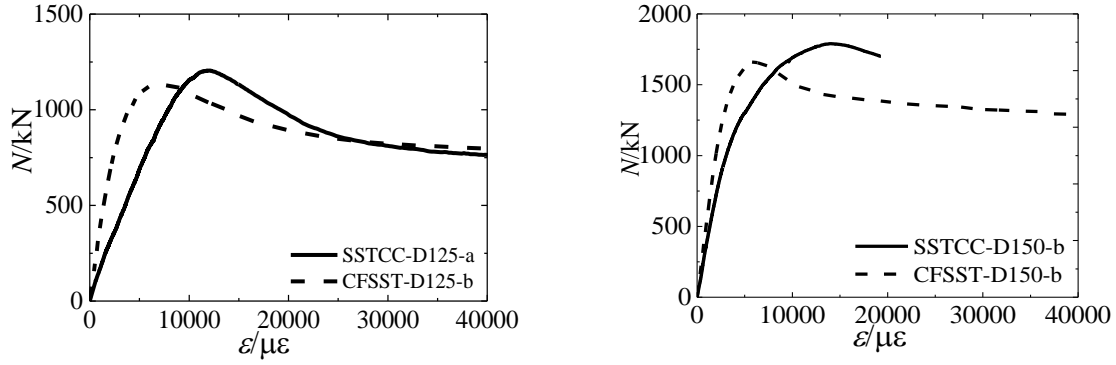
(c) CFSST-D180

Fig.13. Axial strain and load relationship of CFSST stub columns

4.3. Comparison of experimental results

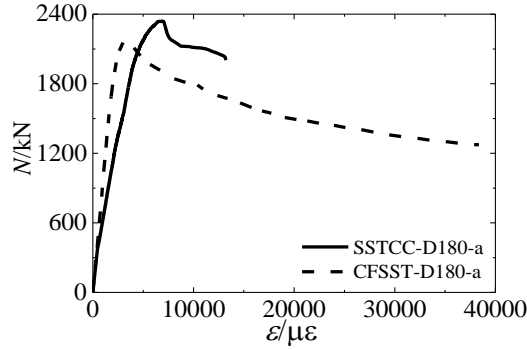
Fig. 14 shows the comparison of SSTCC columns and CFSST columns with same diameter. For SSTCC columns, the core concrete is subjected to compression and the stainless steel tube would not contribute to resist the vertical load directly. While for CFSST columns, the steel tube and core concrete are loaded simultaneously. From Fig. 14, it can be seen that the load-carrying capacity of SSTCC columns is higher than that of CFSST columns. For specimen with diameter-to-thickness ratios of 108, 97 and 90, the increase ratio of load-carrying capacity are 2.5%, 6.4% and 7.5%.

The rigidity of stainless steel tube confined concrete member is obviously lower than that of concrete-filled steel tubes. The rigidity of tube confined concrete member decreases about 20%. In addition, the deformation corresponding to peak load of SSTCC column is larger than that of CFSST column. For tube confined concrete member, in elastic stage, the steel tube has little contribution to the rigidity. While for CFSST columns, the steel tube is mainly to resist vertical load in elastic stage. In the elastic-plastic stage, the hoop stress of tube increases which would decrease the axial compressive stress of steel tube according to Von-Mises criterion.



(a) Specimens with diameter of 125 mm ($D/t=97$)

(b) Specimens with diameter of 150 mm ($D/t=90$)



(c) Specimens with diameter of 180 mm ($D/t=108$)

Fig.14. Comparison between SSTCC and CFSST

5. Axial strength of stainless steel tube confined stub columns

Although the stainless steel tube is not supposed to contribute to the axial resistant to the compressive loading, based on the experimental results, it was found that the stainless steel tube at the mid-height would partially resist the axial load even the stainless steel tube is cut on both ends. This is due to the friction between steel tube and core concrete, which enable the steel tube to take the axial load. The circumference stress on the steel tube would confine the concrete, thus the concrete was under the state of three-directional compression. The compressive strength of confined concrete was proposed by Mander [29]:

$$f_{cc} = f'_c \left(-1.245 + 2.245 \sqrt{1 + 7.94 \frac{f'_r}{f'_{co}} - 2 \frac{f'_r}{f'_{co}}} \right) \quad (11)$$

Where, f'_r is the effective confining stress of circular tube on the concrete, which can be calculated as following:

$$f_r' = \frac{2t\sigma_h}{D-2t} \quad (12)$$

The stainless steel is also assumed to obey the Von-Mises yielding criterion as following:

$$\sigma_z = \sqrt{\sigma_h^2 + \sigma_v^2 - \sigma_h\sigma_v} \quad \text{and} \quad \sigma_z \leq \sigma_{0.2}$$

When the stainless steel reached the yielding stress, it can be assumed that the steel meets the following equation.

$$\sigma_{0.2} = \sqrt{\sigma_h^2 + \sigma_v^2 - \sigma_h\sigma_v} \quad (13)$$

After the axial stress σ_v is known, the corresponding circumference stress σ_h can be calculated according to Eq. (13).

Based on the test results of SSTCC columns, it was found that when the specimens reached their load-carrying capacity, the axial stress on the steel tube is about 60% of yielding stress. According to the Von-Mises criterion, the circumference stress on the steel tube is 0.55 times of yielding stress. Based on the test results of CFSST columns, it was found that the axial stress on the steel tube is about 0.9 times of yielding stress of steel when the specimens reached their load-carrying capacity, and the corresponding circumference stress on the steel tube is 0.18 times of yielding stress. Thus the following equation is suggested to calculate the loading-carrying capacity of stainless steel tube confined concrete stub columns and concrete-filled stainless steel tube stub columns.

$$N_u = f_{cc}A_c + A_s\sigma_v \quad (14)$$

$$\sigma_v = \beta\sigma_{0.2} \quad (15)$$

$$\sigma_h = \frac{\sqrt{4-3\beta^2}-\beta}{2}\sigma_{0.2} \quad (16)$$

In which, β is the proportional factor of axial stress corresponding to the yielding stress of steel; f_{cc} can be calculated by Eq. 11. A_c is the area of core concrete; A_s is the area of steel tube. As analyzed above, the factor β is 0.6 for SSTCC columns while 0.9 for CFSST columns. Using the Eq. 14, the load-carrying

capacities of all specimens are calculated and listed in Table 2. It can be seen that the calculated results are close to the experimental results, indicating that the proposed equation can be used to calculate the load-carrying capacity of stainless steel tube confined concrete members and concrete-filled stainless steel tubes. Also, the capacities of sum of concrete and stainless steel tube are listed in Table 2. It can be seen that the capacity of SSTCC columns are about 34% higher in average than the sum of concrete and steel tube, while the capacity of CFSST columns are about 27% higher in average than the sum of concrete and steel tube. The reason is that the core concrete is confined by stainless steel tube in all columns and the confinement of stainless steel tube in SSTCC columns is larger than that in CFSST columns.

Table 2 Comparison between test results and calculated results

No.	D <i>mm</i>	t <i>mm</i>	Δ_u <i>mm</i>	N_{s+c} <i>kN</i>	N_{ue} <i>kN</i>	N_c <i>kN</i>	N_c/N_{ue}	N_{ue}/N_{s+c}
SSTCC-D125-a	125.3	1.29	3.59	905	1205	1174	0.974	1.33
SSTCC-D125-b	124.8	1.25	3.61	905	1160	1153	0.994	1.28
SSTCC-D125-c	124.5	1.33	3.63	905	1131	1175	1.039	1.25
CFSST-D125-a	124.8	1.31	2.72	905	1131	1047	0.926	1.25
CFSST-D125-b	125.3	1.3	2.72	905	1142	1051	0.920	1.26
SSTCC-D150-a	149.7	1.63	4.67	1305	1759	1650	0.938	1.35
SSTCC-D150-b	149.8	1.67	6.43	1305	1790	1666	0.931	1.37
SSTCC-D150-c	150.2	1.67	3.86	1305	1812	1674	0.924	1.39
CFSST-D150-a	150.1	1.68	2.81	1305	1698	1544	0.910	1.30
CFSST-D150-b	149.8	1.65	2.83	1305	1661	1530	0.921	1.27
SSTCC-D180-a	180.8	1.68	4.14	1730	2340	2275	0.972	1.35
SSTCC-D180-b	180.6	1.65	3.94	1730	2333	2257	0.968	1.35
SSTCC-D180-c	180.7	1.67	4.25	1730	2360	2269	0.961	1.36
CFSST-D180-a	180.7	1.69	2.08	1730	2169	2109	0.972	1.25
CFSST-D180-b	180.7	1.7	2.25	1730	2193	2113	0.963	1.27

Note: Δ_u is the displacement corresponding to the load-carrying capacity; N_{ue} is the capacity of experimental results; N_{s+c} is the sum capacity of steel and concrete; N_c is the calculated capacity of specimen.

6. Conclusions

This paper studied the behavior of axially loaded stainless steel tube confined concrete stub columns

and concrete-filled stainless steel stub columns. The experimental phenomena are introduced in detail.

Based on the analysis of experimental results, the following conclusions can be drawn:

(1) Both stainless steel tube confined concrete stub columns and concrete-filled stainless steel stub columns possess high load-carrying capacity. The load-carrying capacity of stainless steel tube confined concrete members is higher than that of concrete-filled stainless steel stub columns.

(2) The quality of welding is a key factor for steel tube confined specimens, which would influence the deformation ability of the specimens. The seamless steel tubes are suggested to be used for stainless steel tube confined concrete members.

(3) For stainless steel tube confined concrete members, although the stainless steel stub is cut on both ends, the steel tube would still resist certain percentage of the overall vertical load. Based on the test results, the contribution of axial stress of steel tube to the load-carrying capacity should be considered.

(4) A formula to calculate the load-carrying capacity of stainless steel tube confined concrete members is proposed, which is also can be used to calculate the load-carrying capacity of concrete-filled stainless steel stub columns.

Acknowledgements

This research was financially supported by the Jilin Science and Technology Development Project (20180201031SF), the Major (key) Projects of Key R & D Projects in the Ningxia Hui Autonomous Region (2018BEG02009) and the National Natural Science Foundation of China (Grant No. 51778185). The authors wish to acknowledge the sponsors. However, any opinions, findings, conclusions and recommendations presented in this paper are those of the authors and do not necessarily reflect the views of the sponsors.

References

- [1] Liu Jiepeng, Zhang Sumei. Behavior and strength of circular tube confined reinforced-concrete (CTRC) columns. *Journal of Constructional Steel Research*, 2009, 65: 1447-1458.
- [2] Wang Xuanding, Liu Jiepeng, Zhang Sumei. Behavior of short circular tubed-reinforced-concrete columns subjected to eccentric compression. *Engineering Structures*, 2015, 105:77-86.
- [3] Liu Jiepeng, Zhou Xuhong. Behavior and strength of tubed RC stub columns under axial compression. *Journal of Constructional Steel Research*. 2010, 66:28-36.
- [4] Mcateer Peter, Bonacci F., Lachemi Mohamed. Composite response of high-strength concrete confined by circular steel tube. *ACI Structural Journal*, 2004, 101(5):466-474.
- [5] Hong Mei, Kiousis, Ehsani MR, Saadatmanesh H. Confinement effects on high-strength concrete. *ACI Structural Journal*, 2001, 98(4):548-553.
- [6] Liu Faqi, Yang Hua, Leroy Gardner. Post-fire behaviour of eccentrically loaded reinforced concrete columns confined by circular steel tubes. *Journal of Constructional Steel research*, 2016, 122:495-510
- [7] Liu Jiepeng, Teng Yue, Zhang Yusong, et al. Axial stress-strain behavior of high-strength concrete confined by circular thin-walled steel tubes. *Construction and Building Materials*, 2018, 177: 366-377.
- [8] Liu Faqi, Leroy Gardner, Yang Hua. Post-fire behaviour of reinforced concrete stub columns confined by circular steel tubes. *Journal of Constructional Steel Research*, 2014, 102:82-103.
- [9] Wang Xuanding, Liu Jiepeng, Zhou Xuhong. Behaviour and design method of short square tubed-steel-reinforced-concrete columns under eccentric loading. *Journal of Constructional Steel Research*, 2016, 116:193-203.
- [10] Liu Jiepeng, Wang Xuanding, Zhang Sumei. Behavior of square tubed reinforced-concrete short columns subjected to eccentric compression. *Thin-Walled Structures*, 2015, 91:108-115.

393 [11] Zhou Xuhong, Yan Biao, Liu Jiepeng. Behavior of square tubed steel reinforced-concrete (SRC)
394 columns under eccentric compression. *Thin-Walled Structures*, 2015, 91:129-138.

395 [12] Young B, Ellobody E. Experimental investigation of concrete-filled coldformed high strength stainless
396 steel tube columns. *Journal of Constructional Steel Research*, 2006, 62(5):484–492.

397 [13] Ellobody E, Young B. Design and behavior of concrete-filled cold-formed stainless steel tube columns.
398 *Thin-Walled Structures*, 2007, 45(3):259-273.

399 [14] Ellobody E, Young B. Design and behaviour of concrete-filled cold-formed stainless steel tube
400 columns. *Engineering Structures*, 2006, 28:716–728.

401 [15] Dennis Lam, Leroy Gardner. Structural design of stainless steel concrete filled columns. *Journal of*
402 *Constructional Steel Research*, 2008, 64(11):1275-1282.

403 [16] Hassanein, M.F., Kharoob O.F. and Liang Q.Q. Circular concrete-filled double skin tubular short
404 columns with external stainless steel tubes under axial compression. *Thin-Walled Structures*, 2013,
405 73:252-263.

406 [17] Suliman Abdalla, Farid Abed, Mohammad AlHamaydeh. Behavior of CFSTs and CCFSTs under
407 quasi-static axial compression. *Journal of Constructional Steel Research*, 2013, 90(5):235-244.

408 [18] Ye Yong, Zhang Shijiang, Han Linhai, et al. Square concrete-filled stainless steel/carbon steel
409 bimetallic tubular stub columns under axial compression. *Journal of Constructional Steel Research*,
410 2018, 146:49-62.

411 [19] Han Linhai, Ren Qingxin, Li Wei. Tests on stub stainless steel–concrete–carbon steel double-skin
412 tubular (DST) columns. *Journal of Constructional Steel Research*, 2011, 67(3):437-452.

413 [20] Wang Facheng , Han Linhai, Li Wei. Analytical behavior of CFDST stub columns with external
414 stainless steel tubes under axial compression. *Thin-Walled Structures*, 2018, 127: 756-768.

- [21] Feng Ran, Chen Yu, Wei Jiangang, et al. Experimental and numerical investigations on flexural behaviour of CFRP reinforced concrete-filled stainless steel CHS tubes. *Engineering Structures*, 2018, 156: 305-321.
- [22] Chen Yu, Feng Ran, Shao Yongbo, et al. Bond-slip behaviour of concrete-filled stainless steel circular hollow section tubes. *Journal of Constructional Steel Research*, 2017, 130:248-263.
- [23] Chen Yu, Wang Kai, Feng Ran, et al. Flexural behaviour of concrete-filled stainless steel CHS subjected to static loading. *Journal of Constructional Steel Research*, 2017, 139:30-43.
- [24] Chen Yu, Feng Ran, Wang Lipeng. Flexural behaviour of concrete-filled stainless steel SHS and RHS tubes. *Engineering Structures*, 2017, 134:159-171.
- [25] GB/T 228-2002. Metallic materials-Tensile testing at ambient temperature. Beijing, China; 2002
- [26] GB/T 50081-2002. Standard for test method of mechanical properties on ordinary concrete. Beijing, China; 2002.
- [27] Quaeh W M, Teng J G, Chung K F. Three-Stage Full-Range stress-Strain Model for Stainless Steels. *Journal of Structural Engineering ASCE*, 2008, 134 (9):1518-1527.
- [28] Zhang Sumei, Guo Lanhui, Ye Zaili and Wang Yuyin. Behavior of steel tube and confined high strength concrete for concrete-filled RHS tubes. *Advances in Structural Engineering*, 2005, 8(2):101-116.
- [29] Mander JB, Priestley MJN, Park R. Theoretical stress-strain model for confined concrete. *Journal of the Structural Engineering*, 1988, 114(8):1804-1826.